AAPS PharmSciTech (2024) 25:180
https://doi.org/10.1208/s12249-024-02875-x

RESEARCH ARTICLE

Effects and Action Mode of Oleic Acid and Azone on Release and Penetration Process of Levothyroxine Sodium Patches

Xing Li[1] · Kaili Liang[1] · Yingying Dong[2] · Shen Li[2] · Zhengnan Gao[2] · Qing Wang[1]

Received: 26 April 2024 / Accepted: 18 June 2024 / Published online: 6 August 2024

Abstract

In recent years, there has been a significant increase in the prevalence of thyroid diseases, particularly hypothyroidism. In this study, we investigated the impact and mechanisms of Chemical permeation enhancement(CPE) on transdermal permeation of levothyroxine sodium (L-T4) patches.We found that the combination of oleic acid (OA) and Azone (NZ) yielded the best transdermal permeation effect for L-T4.Subsequently, we also investigated the relevant propermeability mechanism. The results demonstrate that the combined application of OA and NZ significantly enhances the transdermal permeation of L-T4 compared to individual applications,it is attributed to two mechanisms: firstly, OA improves drug release by increasing the flowability of the pressure-sensitive adhesive (PSA) matrix; secondly, both OA and NZ act on the stratum corneum, especially facilitating L-T4 permeation through the hair follicle pathway. No skin irritation or cytotoxicity is observed with these final patches, which exhibit a remarkable therapeutic effect on hypothyroidism. this study contributes to the development of transdermal formulations of L-T4.

Keywords chemical penetration enhancers · hypothyroidism · levothyroxine sodium · permeation mechanism · transdermal administration

Introduction

Hypothyroidism is characterized by inadequate production of thyroid hormones by thyroid follicular cells, resulting in a deficiency of these hormones [1, 2]. The preferred treatment approach involves monotherapy with levothyroxine sodium [3]. The fundamental principle of treatment is to supplement thyroid hormones by administering exogenous thyroxine (T4), which converts to the active metabolite triiodothyronine (T3) in peripheral tissues [4]. L-T4 can also be utilized for suppressive therapy following thyroid cancer surgery, non-toxic thyroid nodules (with normal thyroid function), prevention of thyroid nodule recurrence after post-thyroidectomy, female infertility with elevated thyroid antibodies, obesity management, and depression treatment, among other indications [5]. However, instances of under-treatment or over-treatment are not uncommon, highlighting the necessity for precise dosing [6]. Currently, monotherapy with oral levothyroxine sodium remains the favored treatment for hypothyroidism [7]. Nevertheless, factors such as stomach pH [8], gastrointestinal diseases [9], or dietary soy etc. [10–13] have been identified as potential interferences with levothyroxine sodium absorption. Based on this, the requirements for the frequency and time of administration of L-T4 are rigid and strict [14]. It should be taken 1 h before fasting breakfast every day, and the interval between taking other drugs should be more than 4 h, which brings limitations to oral administration. In such situations, there arises an urgent need for a convenient and long-lasting alternative.

Transdermal drug delivery systems (TDDS) utilize the skin as a pathway for drug administration and represent the third generation of pharmaceutical preparations, ranking just below oral and injectable formulations [15, 16]. This method of administration is convenient, user-friendly, non-invasive, and reduces dosing frequency through sustained-release

✉ Zhengnan Gao
gao2008@dlut.edu.cn

✉ Qing Wang
qwang@dlut.edu.cn

[1] Dalian University of Technology, No. 2 Linggong Road, Ganjingzi District, Dalian 116024, Liaoning, P. R. China

[2] Central Hospital affiliated to University of Science and Technology, Dalian 116021, P. R. China

formulations, improving patient compliance [17]. TDDS also minimizes fluctuations in drug concentration in the blood, maintains stable plasma levels, and reduces the risk of overmedication [18, 19]. Additionally, it avoids the gastrointestinal environment, including pH levels, enzyme activity, drug-food interactions, and the hepatic "first-pass effect" that can interfere with drug efficacy [20]. TDDS can effectively address the limitations of oral levothyroxine sodium preparations. Stewart SA *et al*. [21] have explored subcutaneous implants based on polyethylene glycol for continuous delivery of levothyroxine sodium, achieving a treatment duration of up to four weeks. Ghazi RF *et al*. [22] developed a subcutaneous implant based on polycaprolactone for sustained release of levothyroxine sodium, enabling treatment to last up to four weeks. However, both microneedles and subcutaneous implants employ physical enhancement methods that may potentially compromise patient adherence.

In the preparation of patches, the choice of matrix type is crucial. Polyacrylate PSA is one of the most important and widely used types in PSAs [23]. Its advantages, including excellent adhesion, mechanical properties, chemical stability, good drug miscibility, non-toxicity, and low cost, make it widely employed in patch preparation [24, 25]. The simplest form of PSA patches is the drug-in-adhesive (DIA) type, where the drug is directly dissolved or dispersed in the PSA polymer [26]. Drug-containing PSA matrices serve various functions, including skin adhesion, drug storage, and control of the permeation rate of drug penetration enhancers. They also regulate the distribution of the active ingredient in the stratum corneum, making them a convenient and effective matrix type.

Levothyroxine sodium (798.86 D) is limited by its relatively large molecular weight, making it challenging to achieve complete skin penetration without any enhancement methods. CPE is an effective approach that uses relatively inert chemical substances to assist in transdermal drug absorption [27–29]. The mechanism of action of CPE typically involves acting on the stratum corneum, which reduces the resistance provided by intracellular keratin and intercellular lipid regions. Indirect effects include optimizing the thermodynamic activity of the drug, influencing the drug's distribution coefficient, increasing its solubility in the carrier, and forming a reservoir for the drug in the skin [30–33]. The combined use of CPE is often more effective than individual application in enhancing percutaneous penetration [34]. For example, Hiroki Saitoh *et al*. [35] that the combined application of OA and Tween 80 further enhanced the absorption-promoting effect of DSF compared to individual application. Ramesh Panchagnul *et al*. [36] studied the effect of water, ethanol and propylene glycol on the penetration of naloxone *in vitro*, and the results showed that the use of the two-part combination of ethanol and propylene glycol could improve the penetration effect of naloxone. Therefore, the combined use of enhancers is a promising approach.To enhance the transdermal penetration of L-T4 for improved therapeutic efficacy, an appropriate amount of CPE should be included in the prescription.

In the treatment of diseases such as hypothyroidism requiring long-term medication, transdermal formulations with continuous administration and reduced dosing frequency have significant efficacy. Therefore, this study developed a transdermal delivery formulation of levothyroxine sodium with good permeation effects. OA and NZ were determined to have enhancing effects on the release and permeation of levothyroxine sodium in PSA patches. The mechanism of action was validated through rheometers, attenuated total reflection fourier transform infrared spectroscopy (ATR-FTIR), Raman spectroscopy (CRM), scanning electron microscopy (SEM), and other instruments. The combined use of penetration enhancers improved the transdermal permeation of L-T4, achieving prolonged release on the skin and overcoming the challenges of variable bioavailability associated with oral administration, better meeting the clinical treatment needs.

Materials and Methods

Materials

Reagent

Levothyroxine sodium (purity ≥ 98%) was purchased from Tianjin Xi enshi Biochemical Technology Co., Ltd (Tianjin, China). Trifluoroacetic acid was purchased from Macklin Biochemical Co., Ltd (Shanghai, China). Acetonitrile and methanol are both purchased from Thermo Fisher Scientific China Co., Ltd (Shanghai, China). Pressure sensitive adhesive DURO-TAK 2852 was purchased from Henkel Chemical Co., Ltd (New Jersey, USA). OA (purity ≥ 65%) was purchased from Aladdin Biochemical Technology Co., Ltd (Shanghai, China). NZ was purchased from Aladdin Biochemical Technology Co., Ltd (Shanghai, China).Propanediol (PG) was purchased from Elkem Pharmaceuticals Co., Ltd (Hunan, China). Isopropyl myristate (IPM) was purchased from CRODA International Plc (Snaith, UK). Plurol Oleique CC497 (POCC) was purchased from Tianrun Pharmaceutical Co., Ltd (Guangzhou, China). Ethyl acetate and PEG400 are both purchased from China National Pharmaceutical Group Chemical Reagent Co., Ltd (Jiangsu, China). Propylthiouracil (PTU) (purity ≥ 98%) was purchased from Shanghai Macklin Biochemical Co., Ltd. (Shanghai, China). Euthyrox was purchased from Merck Healthcare (Darmstadt, Germany). Cyanate ester adhesive was purchased from H.B. Fuller (Dublin, Ireland). MTT reagent kit was purchased from KGI Biotechnology Co., Ltd (Jiangsu, China). T4 assay

kit was purchased from Shanghai Jining Industrial Co., Ltd (Shanghai, China).

Animal

The experimental animals used in this study include healthy SD (Sprague Dawley) rats (SPF, male, 200 ± 20 g, **6 weeks)**, BALB/c Hair-less mouse (SPF, male, approximately 20 ± 2 g, **6 weeks**), KM (Kunming) mice (SPF, male, approximately 20 ± 2 g,**4 weeks**), NZW rabbits (New Zealand White rabbits) (SPF, male, 2500 ± 100 g, **3 months**) All experimental animals for this study were provided by Liaoning Changsheng Biotechnology Co., Ltd. (China, Liaoning). The research involving all experimental animals was conducted in accordance with the guidelines for the welfare of experimental animals at Dalian University of Technology (Approval Number: DUTSCE220813_01).

Preparation of Skin

Healthy SD rats, BALB/c hair-less mouse, and KM mice were euthanized by cervical dislocation,and then fixed on experimental board. The back fur was removed using a depilatory knife, and peeled off using a toothless forceps and surgical scissors. Pay attention to removing subcutaneous fat and connective tissue from the skin. The back was repeatedly washed with sterile 0.9% sodium chloride solution. The integrity of the skin was observed under a microscope (Olympus CX43, Japan). Pig skin **(Bama pig, male, 30 days)** purchased from Linxi County Jingde Agricultural Products Sales Co., LTD. (Hebei, China).The prepared samples were sealed in bags and stored at -20°C for later use.

HPLC Analysis

The L-T4 content was detected using reverse-phase HPLC on a Shimadzu LC-2030 liquid chromatograph. The chromatographic conditions were as follows: Welch Ultimate XB-C18 column (250mm × 46mm, 5 μm, Yue Xu Technology Co., Ltd., China, Shanghai) was employed; the mobile phase consisted of acetonitrile -0.1%TFA (40:60, v/v); detection was performed at a wavelength of 225 nm; the flow rate was set at 1.0 mL/min; an injection volume of 20 μL was used; and the column temperature was maintained at 30°C.

Preparation of Adhesive Drug Patches

The experimental study set the drug loading as 9% wt.Levothyroxine sodium was dissolved in ethyl acetate in a glass beaker, and then PSA (DURO-TAK® 87–2852) and CPE (OA, PG, IPM, POCC, NZ,one or two types) was added. The mixture was homogenized under magnetic stirring for 1 h, and then degassed at room temperature. The resulting drug-containing PSA solution was coated onto a backing layer using a MS-GD300 Automatic blade coater (Maosen Automation Equipment Co., LTD, Xiamen, China). After removal of the solvents in an oven at 60–70°C for 10 min, the film was finally laminated with a backing layer (The backing layer and anti-stick layer both was covered with a PET membrane.). All patches were cut into a suitable size and packaged in aluminum foil before use.

In Vitro Drug Release Study

In vitro drug release experiments were conducted using a Franz vertical diffusion cells (KX-10VPC, Dalian Kexiang Technology Co., Ltd., China) with an effective area of 1.767 cm2 and a receiver volume of 10 mL. The patch backing layer was adhered to transparent tape serving as a support, and it was assembled onto the diffusion cell. The temperature was set at 32°C, and stirring was provided by a magnetic bar at 600 rpm. Samples were taken at 1, 3, 6, 9, 12, 24, and 27 h. A 200 μL sample was extracted and supplemented with blank receiving solution (40% PEG400-water solution) of the same volume and temperature. After centrifugation, the supernatant was sucked under the chromatographic conditions mentioned in Section "HPLC Analysis" and the drug cumulative release amount (Q) and release enhancement ratio (ER_R) at each time point were calculated using the following formulas. Cumulative drug release is calculated as follows:

$$Q = \frac{C_n \times V + \sum C_{n-1} \times V_n}{M}$$

wherein, Q: Cumulative drug release (μg/cm^2);M: Diffusion area (cm^2);V: Total volume of the receiving solution (mL);C_n: Measured concentration at various time points (μg/mL);V_n: Sampling volume (mL).

IVPT Study of L-T4 Saturated Solution

The *in vitro* skin permeation experiment was conducted using a Franz horizontal diffusion cells(KX-5HPC, Dalian Kexiang Technology Co., Ltd, China) with an effective area of 0.785 cm2, where the volumes of the supply and receiving cells were 5 mL. Before the experiment, rat skin was naturally thawed at room temperature and fixed between the two cells, with the stratum corneum facing the supply cell and the dermis facing the receiving cell. Subsequently, blank receiving solution was added to the receiving cell, and the system was incubated at 32 ± 0.5 ℃ with a rotation speed of 600 rpm for 30 min.

Following this, levothyroxine sodium-saturated 40%(v/v) PEG400-water solution and 5% CPE were added into the donor compartment and mixed well. At 1, 3, 6, 9, 12, 24, 48,

and 72 h after the start of the experiment, 200 µL solution was drawn from the receiving pool and an equal volume of blank receiving solution was added. After centrifugation, the supernatant was taken for chromatographic analysis under the conditions specified in "HPLC Analysis" The cumulative drug transdermal permeation amount (R) and transdermal absorption enhancement ratio (ER_P) were then calculated.

The formula for calculating the cumulative drug transdermal permeation amount is as follows:

$$R = \frac{C_n \times V + \sum C_{n-1} \times V_n}{A}$$

wherein:R:the cumulative permeation amount (µg/cm2);V:the total volume of the receiving solution (mL);C_n:the measured concentration at each time point (µg/mL);V:the sampling volume (mL);A:the diffusion area (cm2);

IVPT Study of L-T4 Patch

An *in vitro* permeation experiment of patches was conducted using a vertical diffusion cell (KX-10VPC, Dalian Kexiang Technology Co., Ltd., China) with an effective area of 1.76 cm2 and a receiving cell volume of 10 mL. Before the experiment, rat, mouse, and L-T4 patches with CPEs skin were thawed naturally at room temperature and fixed between two cells. The stratum corneum faced the donor cell, and the dermis faced the receiving cell. Subsequently, patches were cut to an appropriate size and applied to the skin with the stratum corneum facing up. The experiment was carried out at 32 ± 0.5 ℃ and 600 rpm. Other procedures were consistent with those outlined in 2.5.

Measurement of Drug Concentration in Skin

Experiments were conducted using a vertical diffusion cell and excised pig skin. L-T4 patches without CPEs patches and L-T4 patches with CPEs were used for a 72-h *in vitro* permeation study. At the end of the experiment, the receiving fluid was taken from the diffusion cell, and the L-T4 content was analyzed using HPLC. The skin was removed from the diffusion cell and placed onto a flat surface with the stratum corneum (SC) facing up. The skin was cleaned with a water-soaked gauze pad and tape-stripped 15 times, using tapes. L-T4 content in the tapes was determined as described below after exhaustive extraction of the drug with methanol over a 24 h period. A drop of cyanoacrylate superglue was applied to the stripped skin area and covered with an additional tape-strip using light pressure. After complete polymerization of the glue (5 min), this tape-strip was then removed, and the skin surface biopsy obtained in this way contained hair follicles casts, from which L-T4 was extracted with methanol and quantified by HPLC.

Influence of CPE on L-T4 Patch Properties

ATR-FTIR Analysis

Fourier transform infrared spectroscopy (Nicolet IS50, Thermo Scientific, USA) was employed to study the interaction of OA, L-T4, and PSA in patches. L-T4, PSA patches, L-T4 patches without CPEs, and L-T4 patches with CPEs with different proportions of OA were prepared. Scans were conducted at a resolution of 4 cm¯1 within the range of 400–4000 cm¯1.

Rheological Study

Rheological experiments were conducted using a rotational rheometer (HAAKE MARS iQ, Thermo Scientific, USA) to validate the influence of OA on PSA performance. PSA patches, L-T4 patches without CPEs, and L-T4 patches with CPEs with a thickness of 400 ± 10 µm were used as samples after removing the anti-stick and backing layers. All tests were performed at a 400 µm gap and a temperature of 32 ± 1°C. The linear viscoelastic region (LVR) was determined by strain scanning from 0.1% to 100% at a constant frequency of 1 Hz. Frequency scanning was conducted at 1% strain within the LVR, ranging from ω = 0.1 to 100 rad/s. G', G'', and tan(δ) were determined based on angular frequency (ω).

DSC Analysis

DSC measurements were conducted using a DSC-1 instrument (DSC 214 Polyma, NETZSCH, Germany) on PSA patches, L-T4 patches without CPEs, and L-T4 patches with CPEs with different proportions of OA. Samples were placed in aluminum pans and heated from -80°C to 20°C at a rate of 5°C/min. The onset of the inflection point in the DSC thermogram was taken as the T_g value.

Impact of CPEs on the Skin

ATR-FTIR Analysis

Skin penetration experiments were conducted using an *in vitro* vertical diffusion cell. Rat skin was fixed between the supply and receiving cells, with the stratum corneum facing the supply cell. Then, 10 mL of a 40% PEG400-water solution was added to the receiving cell, maintaining the temperature at 32 ± 0.2 ℃. The skin surface underwent the following treatments: 0.8 mL of physiological saline or a

treatment with NZ + OA (1% + 9%) physiological saline solution for 6 h.

After the experiment, carefully wash the tested skin.The samples were spread on glass slides, placed on a ZnSe ATR crystal with the stratum corneum facing down. ATR-FTIR was used to measure the skin samples' spectra in the range of 400 cm^{-1} to 4000 cm^{-1} with a resolution of 4 cm^{-1}.

CRM Analysis

Raman spectra of skin samples were measured using CRM (inVia Qontor, Renishaw, UK). The skin treatment was similar to ATR-FTIR. The sample measurement parameters were set as follows: excitation wavelength of 780 nm, spectrum scanning range of 400 cm^{-1} to 4000 cm^{-1}, sample exposure time of 15 s, and a measurement depth of the stratum corneum of 0 μm.

SEM Analysis

The skin samples were treated as described in the ATR-FTIR study. After the experiment, the test skins were carefully washed and cut into 5 mm × 5 mm pieces. These samples were fixed with 2.5% glutaraldehyde in PBS (pH 7.0) for 12 h and then washed three times in PBS (pH 7.0) for 5 min at each step; next, they were postfixed with 1% OSO_4 in PBS for 1.5 h and washed three times in PBS (pH 7.0) for 15 min at each step. The samples were dehydrated by a graded series of ethanol (30%, 50%, 70%, 80%, 90%, 95%, and 100%) for 15 min at each step; then, they were transferred to a mixture of ethanol and iso-amyl acetate (v:v = 1:1 for 0.5 h, followed by transfer to pure iso-amyl acetate overnight. Finally, the skins were dried with N_2 to remove the residual solvent and glued to the conductive tape. The samples were then coated with gold in the ion-sputtered sample stage (Q150T ES, UK) for 40 s and visualized under the Quanta 450 SEM (FEI, USA).

Safety Study

MTT Assay

(1) Preparation of test solutions

Precisely weigh 15 mg of L-T4 and place it in a 10 ml volumetric flask. Add sterile PBS solution to the mark. Take 1 ml and dilute it 100 times to obtain a 0.15 mg/ml test solution, then dilute it sequentially to 0.12, 0.09, 0.05, and 0.03 mg/mL. Precisely weigh 15 mg of L-T4, 15 mg of OA, and 1.67 mg of NZ in a 10 ml volumetric flask. Add sterile PBS solution to the mark. Take 1 ml and dilute it 100 times to obtain a test solution containing the penetration enhancer, then dilute it sequentially to 0.12, 0.09, 0.05, and 0.03 mg/mL.

(2) MTT assay

Add human keratinocyte (HaCaT) cells (Beina Biotechnology Co., Ltd.China, HeBei) at 100μL/well (about 1 × 104 cells) to a 96-well plate and incubate in a cell culture incubator at 37℃ with 5% CO_2 for 24 h. Add the prepared concentration of samples. Incubate the 96-well plate in a cell culture incubator at 37℃ with 5% CO_2 in air and 100% humidity for an appropriate time. Add 50 μL of 1 × MTT to each well and incubate at 37℃ for 4 h to reduce MTT to formazan. Remove the supernatant, add 150μL of DMSO to dissolve the formazan in each well, and shake on a plate shaker. The optical density of each well is detected at a wavelength of 490 nm using an enzyme marker at 490 nm.

Cell viability is expressed as:

$$\text{Cell viability} = \frac{T}{C} \times 100\%$$

wherein: *T*:the OD value of the treated cells, *C*:the OD value of the control cells.

Skin Irritation Test

New Zealand white rabbits were used to verify that the patch produced skin irritation. The experimental animals were divided into normal group and damaged group, 4 in each group (half male and half female). The study used a left–right self-contrast method. The back was shaved with electric scissors 24 h before administration, and the damaged skin group used a syringe needle to damage the experimental area skin. PSA patches (4 cm^2), L-T4 patches without CPEs (4 cm^2), and L-T4 patches with CPEs (4 cm^2) were applied separately, and the administration time was 72 h. Redness and swelling symptoms were observed at 0.5, 1, 24, 48, and 72 h after patch removal. After the experiment, the rabbits were euthanized, and the skin at the site of treatment was collected. The samples were washed three times with PBS (0.1 M, pH 7.4) and fixed with 4% formaldehyde solution. The tissues were then embedded in paraffin and subjected to H&E staining.

Pharmacological Study

The hypothyroidism rat model was established using the PTU method. Rats were fed with a 0.1% PTU solution, and the success of the model was confirmed through thyroid histopathological sections and blood T4 levels. Twenty four male SD rats were successfully modeled and randomly divided into four groups: the hypothyroidism group, oral Euthyrox group (1 μg/100 g/d), L-T4 patches without CPEs group

(2.7 cm^2/100 g/3 d), and L-T4 patches with CPEs group ((2.7 cm^2/100 g/3 d). After the rats were anesthetized, the abdominal hair was carefully removed to expose the appropriate area. After 24 h of normal feeding, skin damage in the model area was inspected. The patches were cut to the appropriate size, applied to the rat's abdomen, and secured with gauze and medical adhesive tape. The hypothyroidism group received no treatment. The patches were replaced every 72 h, and approximately 200 µL of blood was collected via the retro-orbital plexus at the 2nd, 4th, and 8th weeks. After centrifugation at 3000 rpm at room temperature, serum was collected, and T4 levels were measured using an enzyme-linked immunosorbent assay (ELISA). Thyroids of the rats were dissected at weeks 0, 2, 4, and 8 for H&E staining and observation of thyroid histopathological sections.

Statistical Analysis

Statistical analysis of samples was carried out with SPSS 21.0, and values were presented as means ± standard deviation of at least three independent determinations. *P*-values were obtained using the two-tailed unpaired student T-test or one-way analysis of variance. Results were determined to be statistically significant as $p < 0.05$.

Results and Discussion

Prescription Screening Results

We assessed the release of L-T4 from patches and the permeation of saturated L-T4 solution using five varying CPEs. Figure 1a illustrates the enhancement effects of OA, PG, NZ, POCC, and IPM at 5%wt on the release of levothyroxine sodium (L-T4) from PSA matrix. The findings demonstrate that all five CPEs significantly enhance the release effect compared to the control group, specially OA exhibits the most potent permeation-enhancing effect on L-T4 by increasing L-T4 release with about 1.6 times.

Typically, studying the permeation of drug-saturated solutions can provide a more accurate demonstration of

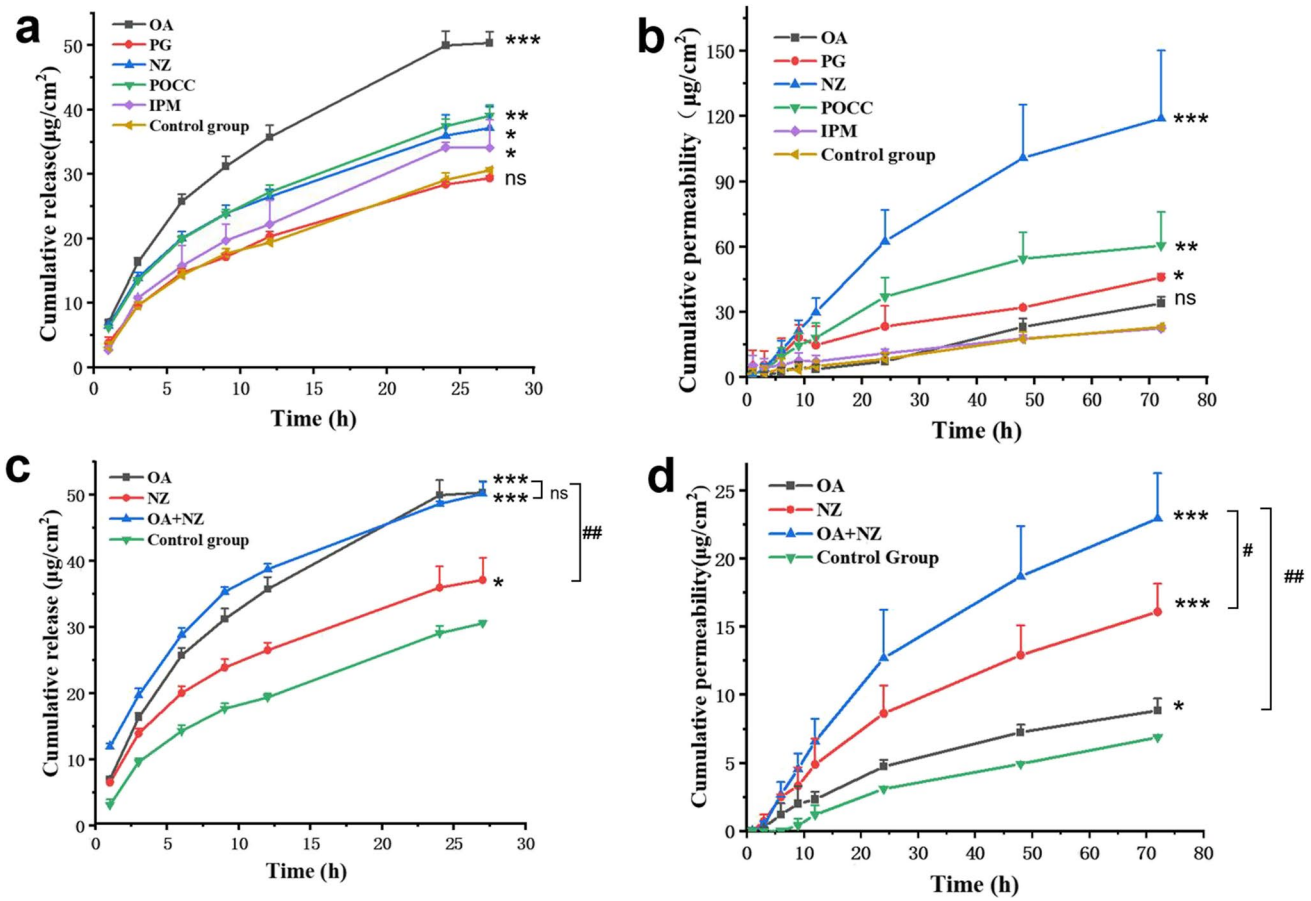

Fig. 1 Screening of CPEs. **a** Release of adhesive with different CPEs; **b** Permeation of saturated L-T4 solution with different CPEs; **c** Release of L-T4 adhesive co-used with OA and NZ; **d** Permeation of L-T4 adhesive co-used with OA and NZ (mean ± SD, $n = 4$, Compared to the control group, $p < 0.001$, ***, $0.001 < p < 0.01$,**,$0.01 < p < 0.05$,*,$p > 0.05$,ns)

the permeation effect, eliminating any interference from the patch matrix. Therefore, we further assessed the impact of these CPEs on drug-saturated solutions. As depicted in Fig. 1b, compared to the control group, NZ significantly enhances the cumulative permeation of L-T4 by 5.137-fold.

Since both drug release and penetration may affect drug transdermal absorption and based on the experimental results described above, NZ and OA were selected as CPE to conduct percutaneous penetration studies of L-T4 (Fig S1). The results of this patch formulation are depicted in Fig. 1c and d. The cumulative drug release at 27 h for the OA + NZ group was found to be 50.385 ± 1.724 μg/cm^2, while it was 50.218 ± 1.831 μg/cm^2 for the OA group and 37.164 ± 3.322 μg/cm^2 for the NZ group (Fig. 1c). Notably, compared to the NZ group alone, co-administration of OA with NZ did not further enhance drug release from the matrix (Fig. 1c), but the cumulative drug permeation at 72 h is significantly enhanced in the OA + NZ group (22.976 ± 3.312 μg/cm^2) compared to the NZ group (16.107 ± 2.076 μg/cm^2),therefor OA and NZ thus showed significant synergistic transdermal promoting effect in L-T4 patch by the different action mechanisms for L-T4 percutaneous absorption.

Enhancement Effect of OA and NZ on L-T4 in Different Skin

To further investigated the synergistic effect of OA and NZ, we conducted experiments to evaluate their penetration in different types of skin. Figure 2a shows the penetration curves of L-T4 patches in different skin. It can be observed that L-T4 exhibited better *in vitro* penetration in rat and mouse skins, while its penetration in hair-less mouse was notably lower with values of 62.732 ± 19.837, 22.976 ± 3.312, and 1.543 ± 0.196μg/cm^2, respectively. Figure 2b demonstrates that a significant permeation enhancement *in vivo* for L-T4 patches with CPEs. however, no notable difference was observed in hair-less mouse. Figure 2c indicated higher enhancement ratios in rat (4.24) and mouse (5.47) skins compared to hair-less mouse skin (1.67), The results indicate a significant increase in *in vitro* penetration of L-T4 patches with CPEs compared to L-T4 patches without CPEs in rat and mouse skins, while no significant difference was observed in hair-less mouse.Reasonable speculation is that the large molecular weight of L-T4 (798.86 D) prevents it from passing through the intact stratum corneum [37]. However, L-T4 exists in an ionized state within the PSA matrix, and under normal circumstances, drug ionization favors penetration through the follicular pathway [38]. Therefore, L-T4 primarily penetrates through the follicular

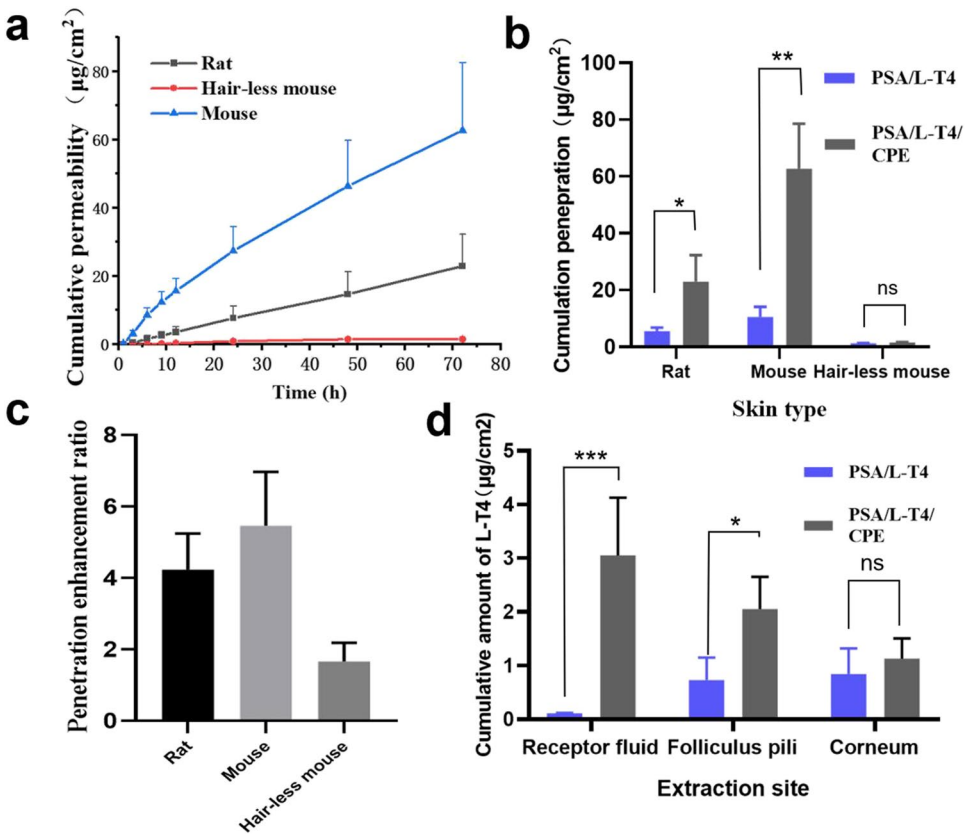

Fig. 2 Penetration effect of patches with CPEs. **a** Penetration curves of patches with CPEs; **b** Cumulative penetration of patches; **c** Enhancement ratio of patches; **d** Drug content in different parts of porcine skin. (mean ± SD, $n = 4$, Compared to the L-T4 patches without CPEs group, $p < 0.001$, ***, $0.001 < p < 0.01$,**,$0.01 < p < 0.05$,*,$p > 0.05$,ns)

pathway of the skin, and CPEs can enhance this route of penetration.

Through cyanoacrylate superglue, we determined the drug content in various regions of porcine skin after penetration test [39]. As illustrated in Fig. 2d, it was indicated that L-T4 patches with CPEs exhibited approximately 3.08 μg/cm^2 penetration in porcine skin, which was significantly different from the L-T4 patch without CPEs. however, there were no statistically significant differences observed in drug content within the stratum corneum. These results demonstrate that co-application of CPEs enhances L-T4 penetration into hair follicles.The results are consistent with *in vitro* penetration outcomes across different skins.

In summary, our findings indicate that L-T4 primarily permeates through the hair follicles pathway, with a minor fraction traversing via the transcorneal route. The cumulative penetration results of L-T4 patches across different skin types suggest that skin thickness, as well as follicle size and quantity, impose limitations on L-T4 penetration. Co-application of CPE significantly enhances the efficacy of L-T4 penetration in hair follicle-containing skin, implying that CPE primarily influences penetration through the hair follicles pathway.

Effect of OA on L-T4 Release

Based on the experimental results of Section "Prescription Screening Results", we found that OA can significantly enhance the release of L-T4 in patch. Therefore, we studied the effects of different OA contents on its release. Figure 3a shows the release and permeation effects of OA contents of 3%, 6%, 9%, and 12% Wt. With the increase of OA content, both the release (i) and permeation effects (ii) of L-T4 increased to a certain extent. The permeation enhancement ratio and release enhancement ratio were linearly correlated (iii), with an R^2 of 0.9374, indicating a good linear correlation, suggesting that OA mainly affects its release, thereby enhancing the penetration of L-T4 into the rat skin [40].

To explore the mechanism of OA increasing the release of L-T4, we conducted rheological tests on the mechanical properties of the drug-containing layer of the patch, as shown in Fig. 3b. The G' value of the PSA patch is always greater than the G" value, and the tan(δ) value is always less than 1, indicating that the PSA matrix has solid-like properties [41]. With the addition of OA, both the elastic modulus and the viscous modulus of the patch matrix were reduced to varying degrees and were lower than the blank PSA layer, indicating a positive correlation with the increase of OA content. The tan(δ) value showed an increasing trend, and the higher the tan(δ) value, the better the flowability of the matrix, which is conducive to the release of small molecules from the matrix [42]. The tan(δ) value was linearly related to the cumulative release, with a good linear correlation, indicating that the addition of OA affects the flowability of the PSA matrix, thereby affecting its release effect.

The infrared characterization results in Fig. 3c show that compared with the PSA and L-T4 patches without CPEs, the addition of L-T4 did not have a significant effect on the matrix. The new peak appearing at 722 cm^{-1} can be attributed to the out-of-plane bending vibration of the amine in L-T4. With the addition of OA, the signal peak at 1340 cm^{-1} is enhanced, which is due to the introduction of alkene structures in the system, representing the in-plane bending vibration of the C = C bond [43]. The signal peak at 722 cm^{-1} first weakened and then increased with the increase of OA concentration, which may be due to the dehydration reaction between the amino group and a small amount of OA first, and then, due to the increase of C = C bonds, the in-plane bending vibration of the alkene structure C-H appeared at the same position. However, no new functional groups between the main peaks (-COOH) in PSA and OA and -NH_2 in L-T4 were observed, and no other interactions between the PSA matrix, drug, and OA were observed, indicating that OA does not affect the release of L-T4 in PSA through chemical bonds.

According to the results of the DSC experiment (Fig. 3e), the Tg values from top to bottom are -53.53, -52.69, -52.86, -52.39, -57.37, and -57.71℃. The addition of the drug increased the Tg value of the matrix, but with the addition of OA, the Tg value gradually decreased, and the curve was smoother compared to the L-T4 patches without CPEs. This result indicates that the addition of OA reduces the Tg value of the matrix, indicating an increase in the flowability of the matrix and improving the compatibility between the drug and the matrix, which is conducive to the release of the drug [44, 45]. This result is consistent with the rheological experiment.

In summary, even a small amount of OA can increase the mobility of the pressure-sensitive adhesive and increases the freedom of L-T4 in PSA, making it easier to move within PSA and thus improving its release effect.

Effects of NZ and OA on Percutaneous Penetration of L-T4

In order to investigate the changes in lipids and keratin in the skin's stratum corneum due to CPE, Fourier-transform infrared spectroscopy experiments were conducted. From the infrared spectrum in Fig. 4a, the -CH_2 stretching bands at ~ 2842 cm^{-1} and 2910 cm^{-1} confirm the trans configuration of hydrocarbons (Fig a i), and the peak at 1725 cm^{-1} indicates the C = O of fatty acids in rat skin (Fig a ii). Changes in peak intensity/area or stretching displacement of characteristic peaks are observed when interacting with lipids in the stratum corneum [46]. After adding the CPE, the symmetric C-H stretching vibration peaks

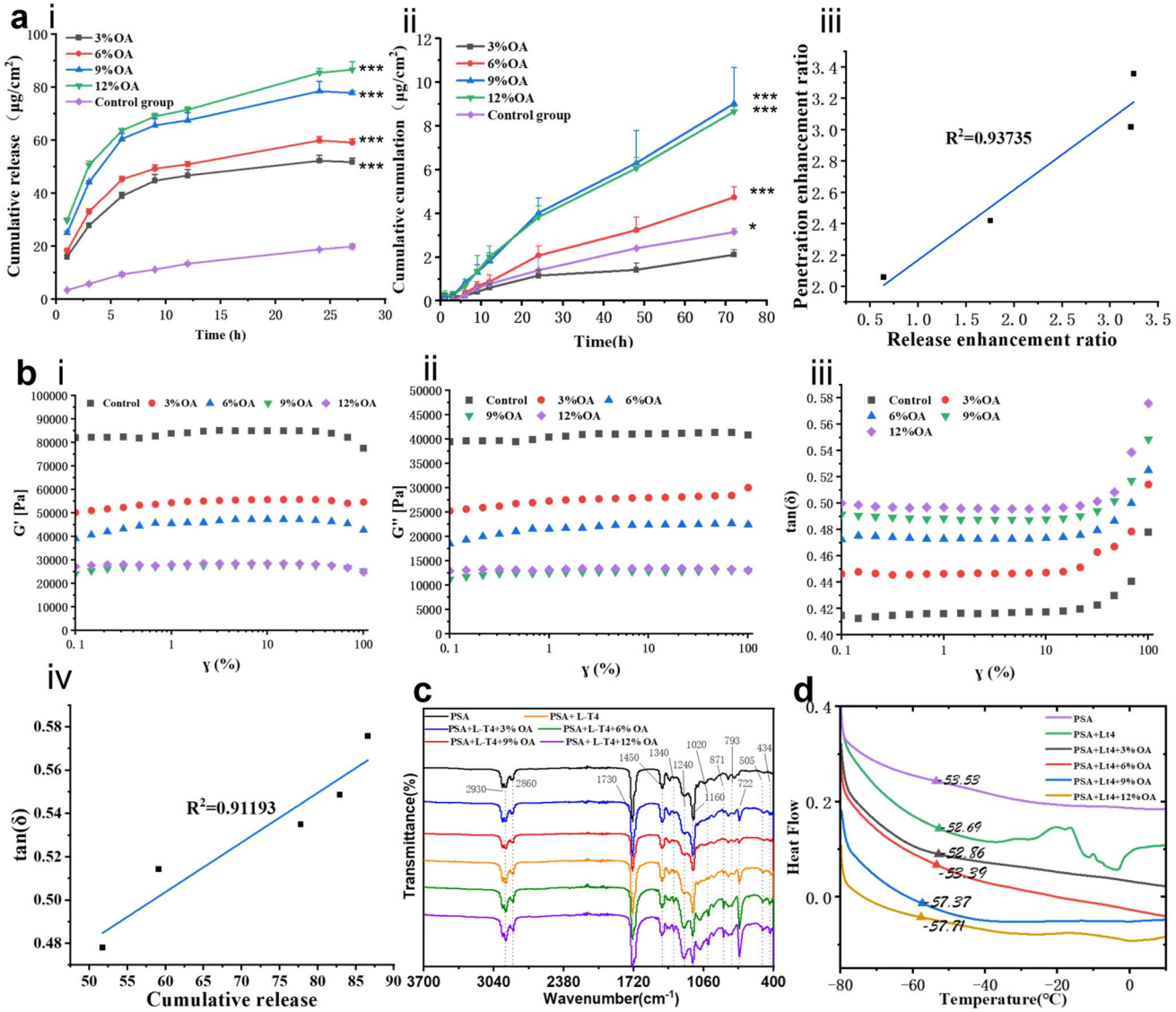

Fig. 3 The Influence of OA on the Release of L-T4. **a** The effects of different OA contents on L-T4. i Effects on release, ii Effects on permeation, iii Fitting curves of release enhancement ratio and permeation enhancement ratio of OA action. **b** Rheological results;i G' values, ii G'' values, iii tan(δ) values, iv Fitting curves of release enhancement ratio and tan(δ) values of OA action. **c** ATR-FTIR results. **d** DSC results (mean ± SD, n = 4, Compared to the control group, $p < 0.001$, ***, $0.001 < p < 0.01$,**,$0.01 < p < 0.05$,*,$p > 0.05$,ns)

(2910.67–2918.78–2922.76 cm^{-1}) and asymmetric C-H stretching vibration peaks (2842.69–2848.87–2851.41 cm^{-1}) both shift to higher wavenumber, while the C = O vibration peak (1725.10–1722.57–1719.10 cm^{-1}) shifts to lower wavenumber. This indicates a transition of the lipid bilayer from an ordered structure to a disordered structure, leading to increased fluidity in lipids [47]. There were no observed changes in the amide region of keratin, as indicated by the absence of alterations in the characteristic absorption peak (NH-C = O at 1544 cm^{-1}) (Fig. S2), suggesting no structural changes in keratin molecules [48].

The Raman spectroscopy in Fig. 4b reflects the conformational changes in lipid molecular chains and the relative intensity changes between conformations, providing a semi-quantitative measure of lipid density in the stratum corneum [49]. In the high wavenumber region (Fig. 4b i), lipid stretching vibrations were observed at V_{asCH_2} 2880 cm^{-1} and V_{sCH_2} 2850 cm^{-1}, along with symmetric stretching vibrations of CH_2 in keratin structure at V_{asCH_2} 2937 cm^{-1}. The higher the ratio of lipid to keratin stretching vibration peak intensity, the more densely packed the lipid structure is, indicating lower permeability. As depicted in Fig. 4b, compared to a

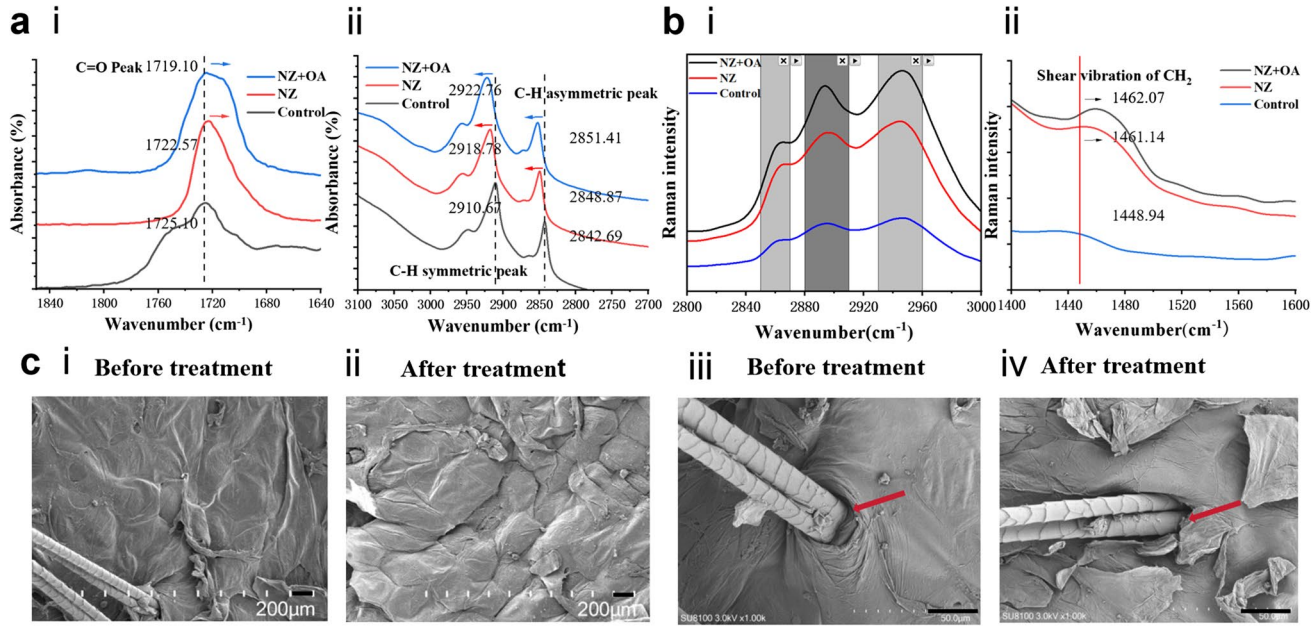

Fig. 4 Effects of NZ and OA on percutaneous penetration of L-T4. **a** ATR-FTIR Results: i -CH_2 Stretching Band, ii C = O of Fatty Acids; **b** CRM Results: i High-Wavenumber Region ii Low-Wavenumber Region; **c** SEM Results: i,iii Physiological Saline Treatment ii,iv OA and NZ Treatment

blank solvent treatment ($AUC_{2883}/AUC_{2937} = 0.9577$), both NZ and NZ + OA treatments resulted in lower AUC_{2883}/AUC_{2937} ratios for stratum corneum samples (0.9048 and 0.9316 respectively).On the other hand, V_{CH_2} 1450 cm^{-1} originates from the scissoring vibration of CH_2 (ii), and its lower wavenumber represents the dense packing of lipids [50]. After NZ and NZ + OA treatments, the stratum corneum samples exhibit higher values (1462.07 and 1461.14, respectively) compared to the sample treated only with a blank solvent (1448.94 cm^{-1}). In summary, the action of NZ + OA can alter the lipid structure in the stratum corneum, making it more loosely packed and promoting drug permeation.

Scanning Electron Microscopy enables visualization of microstructural changes and gaps within the stratum corneum, providing insights into the mechanism by which CPEs act on skin at a microscopic level [51]. Figure 4c illustrates the SEM results. A comparison before and after treatment with NZ + OA shows that the epidermal stratum corneum peels off in sheets (ii), residual layers of keratin around the hair follicle orifice stand upright (iv, red arrow), and keratin near the hair follicle orifice is shed.

In summary, NZ and OA interact with lipids in the stratum corneum, increasing its fluidity and loosening the stratum corneum. Typically, the stratum corneum serves as the primary physical barrier for drug transdermal permeation [52]. However, due to the large molecular weight of L-T4, it cannot penetrate the stratum corneum (as evidenced by *in vitro* percutaneous penetration results in hairless mice), so merely disrupting the stratum corneum is insufficient. Previous reports indicate that NZ can penetrate the skin's stratum corneum and enter the root sheath of hair follicles via the follicular route, interacting with intercellular lipids or biomembrane-like lipids [53–55]. Therefore, NZ leads OA into the hair follicles, where it dissolves lipids to form gaps, enlarging epidermal fissures and widening follicular orifices, thus reducing the diffusion resistance of drugs in the root sheath of hair follicles. Additionally, NZ and OA decrease the ordered arrangement of intercellular lipids, resulting in a loosened stratum corneum, making the outer stratum corneum easier to shed and promoting the shedding of stratum corneum near the follicular orifice. Based on this, CPEs dissolve lipids within the hair follicle and induce the shedding of stratum corneum around the follicular orifice externally, leading to widened follicular orifices, which facilitate the percutaneous penetration of large molecules such as L-T4 through the follicular route.

Safety Evaluation

The utilization of HaCaT cells offers valuable insights into the cytotoxicity of patches and enables a preliminary assessment of their potential skin irritation [56]. As depicted in Fig. 5a, based on the MTT experimental outcomes, NZ, OA, and L-T4 exhibit negligible toxicity towards HaCaT cells, thereby indicating their suitability for use in patches.

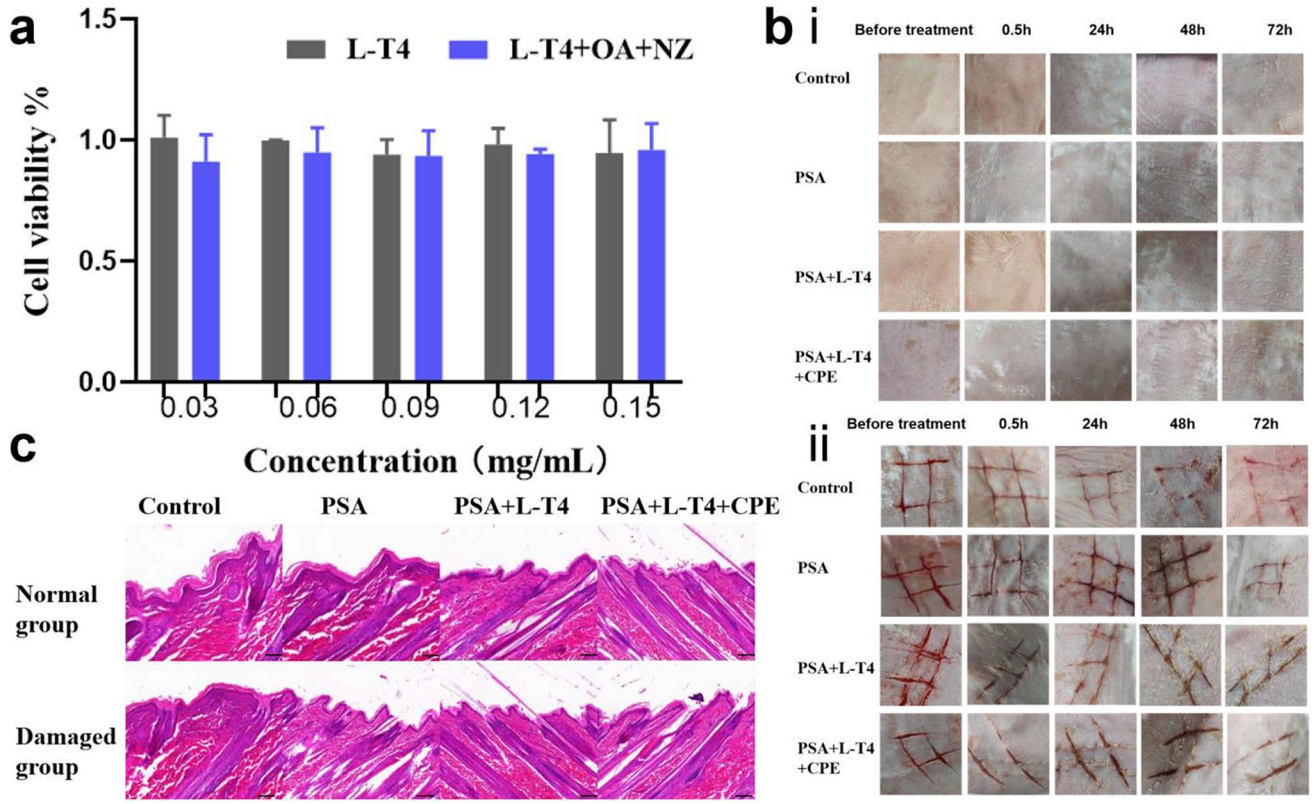

Fig. 5 Safety Evaluation of CPEs. **a** Toxicity of CPEs to Ha-cat Cells; **b** Skin Irritation Results of Patches (i Intact Skin, ii Damaged Skin); **c** Skin Irritation HE Slice Results of Patches (Scale bar = 20 μm)(mean ± SD, $n = 4$)

Skin irritation tests are important indicators of the safety of topical formulations for skin application. As shown in Fig. 5b, after 72 h of administration of OA and NZ, except for the adverse effect of delaying the recovery of rabbit skin lesions by L-T4 patches with CPEs, no obvious erythema or edema reactions were observed in L-T4 patches with CPEs, L-T4 patches without CPEs patches, and PSA patches. In Fig. 5c, no inflammatory reactions were observed in the HE-stained images of rabbit skin, indicating that PSA, L-T4, NZ, and OA have no significant irritant effect on rabbit skin.

Pharmacodynamic Evaluation

Subsequently, we performed pharmacodynamic evaluation of the L-T4 patches with CPEs. We induced hypothyroidism in rats using the PTU method to establish a hypothyroid rat model. In comparison with the T4 level of 33.321 ± 3.691 ng/mL in normal rats, T4 level in hypothyroidism rats reduced to 3.687 ± 1.549 ng/mL (Table I). We observed that the thyroid sections of normal rats were composed of many lobules containing thyroid follicles and parafollicular cells (Fig. 6). Under the light microscope, the thyroid follicles varied in size, with a diameter ranging from 0.02

Table I The Concentration of T4 in Rat Serum (ng/mL)

Item	Normal group	Hypothyroidism group	Oral group	PSA + L-T4	PSA + L-T4 + CPE
0 week	33.321 ± 3.691	3.453 ± 1.187	1.402 ± 0.617	1.726 ± 2.282	1.690 ± 2.379
2 weeks		2.877 ± 1.362	5.161 ± 1.348	8.920 ± 2.122	16.330 ± 3.471$^{###}$
4 weeks		3.399 ± 2.858	13.878 ± 2.311	11.852 ± 5.641	34.257 ± 11.468
8 weeks		3.866 ± 2.164	29.308 ± 10.850	13.507 ± 5.155	32.919 ± 9.245
F	-	0.208	16.880	3.414	13.938
P-value	-	0.889	0.0001***	0.0529	0.0003***

All data were shown in mean ± SD ($n = 4$). Single factor analysis of variance within the group, *, $p < 0.05$; **, $p < 0.01$; ***, $p < 0.001$; Compared to the Oral group,$^{#}$, $p < 0.05$; $^{##}$, $p < 0.01$; $^{###}$, $p < 0.001$

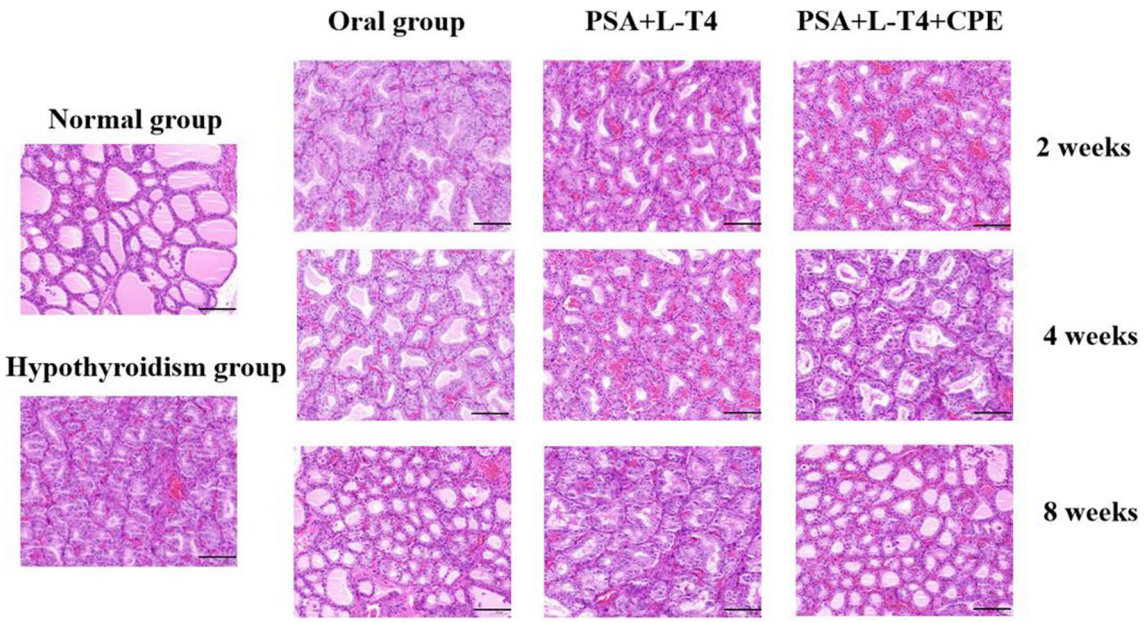

Fig. 6 Pathological sections of rat thyroid (Scale bar = 100 μm)

to 0.9 mm. These follicles appeard round, oval or irregular and were surrounded by a single layer of follicular epithelial cells, consistent with relevant reports [57]. The follicular epithelium was a single layer of cubic epithelium, and the follicular cavity was full of homogeneous eosinophilic colloid, without inflammatory cell infiltration or necrosis. However, the thyroid glands of rats after modeling were red and enlarged by naked eye, significantly larger than the normal group. Under the light microscope, thyroid tissue hyperplasia was observed, follicles became smaller, and the follicular epithelium was tall columnar. Some hyperplasia presented as papillary body protruding into the follicular cavity, and colloid was not seen or rarely seen in the follicular cavity. Some interstitial hyperemia and hemorrhage were observed, indicating that the hypothyroidism model was successfully established.

The pharmacodynamic results are shown in Table I. By one-way analysis of variance within the group, the results showed that the oral group and the L-T4 patches with CPEs group had a significant therapeutic effect. There was no statistically significant difference in the L-T4 patches without CPEs group, although elevated T4 levels were seen *in vivo*. At the second week, the L-T4 patches with CPEs group has shown a stronger therapeutic effect, which is significantly different from the oral group, indicating that the L-T4 patches with CPEs group can have a faster onset of effect. By the fourth week, the levels of thyroid hormone (T4) in rats were increased to 13.878 ± 2.311, 11.852 ± 5.641, and 34.257 ± 11.468 ng/mL for the oral administration group, L-T4 patches without CPEs group, and L-T4 patches with CPEs group, respectively. There was no statistical difference between the oral group and the L-T4 patches without CPEs and L-T4 patches with CPEs groups, but the average (T4) level in the L-T4 patches with CPEs group had reached normal levels and seemed to be better for treatment.These findings highlight both enhanced permeation effects of the L-T4 patches with CPEs formulation and advantages of patch application in avoiding first-pass elimination. With the extension of treatment time, the thyroid hormone (T4) level in the oral group and L-T4 patches with CPEs group basically returned to normal level at the eighth week, while the L-T4 patches without CPEs group had the same effect as the fourth week. The results showed that the addition of osmotic enhancers made the patch have a good effect on hypothyroidism, which is comparable to that of oral preparation.

The pathological sections of rat thyroid glands, as shown in Fig. 6, reveal that the oral Euthyrox group gradually exhibited a clearer structure of thyroid tissue and reduced proliferation compared to the initial state. The thyroid follicles displayed columnar or pseudostratified epithelium and abundant homogeneous colloid within the follicular lumens. The microscopic findings of the L-T4 patches without CPEs group were similar to those of the hypothyroid group, with noticeable follicular dilation, severe follicular vacuolation, and follicular epithelial cell proliferation. However, the microscopic appearance of thyroid tissue in the L-T4 patches with CPEs group was essentially similar to that of the oral Euthyrox group. As time progressed, the phenomena of follicular dilation, vacuolation, and follicular epithelial cell proliferation in rat thyroid tissue decreased, achieving essentially complete recovery from hypothyroidism. Consistent with the results of T4 levels in rats, this indicates the

potential of L-T4 patches with CPEs as an oral substitute formulation.

Conclusion

The combine use of OA and NZ exhibited strong effects to promote both the release and transdermal permeation of L-T4, a synergistic effect was due to increase the release of L-T4 by OA and enhance permeation of L-T4 through the hair follicles pathway by NZ. L-T4 patch as novel route of administration could be selected to address the scarcity of L-T4 formulations. This study provides a valuable technical guidance for the future development of transdermal L-T4 therapy systems.

Supplementary Information The online version contains supplementary material available at https://doi.org/10.1208/s12249-024-02875-x.

Acknowledgements We are grateful to Dalian University of Technology for its instruments and technical support. Thank you for the technical support provided by the Affiliated Central Hospital of Dalian University of Technology.

Author contributions Xing Li: Conceptualization, Methodology, Writing—original draft, Writing—review & editing. The conception and design of the work; The acquisition, analysis, interpretation of data for the work.

Kaili Liang: Conceptualization, Methodology.

Yingying Dong: Data curation, Writing—review & editing.

Shen Li: Writing—review & editing.

Zhengnan Gao: Conceptualization, Project administration, Drafting the work or revising it critically for important intellectual content.

Qing Wang: Final approval of the version to be published.Agreement to be accountable for all aspects of the work in ensuring that questions related to the accuracy of any part of the work are appropriately investigated and resolved.

Funding This work was supported by Medical and industrial cross joint fund project (Award Number:2022ZXYG35)and Liaoning Cancer Hospital and Institute(Award Number: DUT22YG103).

Data Availability The authors confirm that the data supporting the findings of this study are available within the article and/or its supplementary materials.

Declarations

Conflict of Interest There is no conflict of interest in this article.

References

1. Roberts CG, Ladenson PW. Hypothyroidism. Lancet. 2004;363(9411):793–803.
2. Almandoz JP, Gharib H. Hypothyroidism: etiology, diagnosis, and management. Med Clin North Am. 2012;96(2):203–21.
3. Jonklaas J, Bianco AC, Bauer AJ, Burman KD, Cappola AR, Celi FS, et al. Guidelines for the treatment of hypothyroidism: prepared by the american thyroid association task force on thyroid hormone replacement. Thyroid. 2014;24(12):1670–751.
4. Brent GA. Mechanisms of thyroid hormone action. J Clin Invest. 2012;122(9):3035–43.
5. Burlacu MC, Attanasio R, Hegedus L, Nagy EV, Papini E, Perros P, et al. Use of thyroid hormones in hypothyroid and euthyroid patients: a thesis* survey of belgian specialists *thesis: treatment of hypothyroidism in europe by specialists: an international survey. Thyroid Res. 2022;15(1):3.
6. Haas B, Weber-Lassalle K, Frotschl R, Eckstein N. Is sunitinib a narrow therapeutic index drug? - A systematic review and in vitro toxicology-analysis of sunitinib vs. Imatinib in cells from different tissues. Regul Toxicol Pharmacol. 2016;77:25–34.
7. Beck-Peccoz P. Treatment of central hypothyroidism. Clin Endocrinol (Oxf). 2011;74(6):671–2.
8. Virili C, Giovanella L, Fallahi P, Antonelli A, Santaguida MG, Centanni M, et al. Levothyroxine therapy: changes of tsh levels by switching patients from tablet to liquid formulation. A systematic review and meta-analysis. Front Endocrinol (Lausanne). 2018;9:10.
9. Farthing MJ, Rees LH, Edwards CR, Byfield PG, Himsworth RL, Dawson AM. Thyroid hormones and the regulation of thyroid function in men with coeliac disease. Clin Endocrinol (Oxf). 1982;16(6):525–35.
10. Liwanpo L, Hershman JM. Conditions and drugs interfering with thyroxine absorption. Best Pract Res Clin Endocrinol Metab. 2009;23(6):781–92.
11. Campbell NR, Hasinoff BB, Stalts H, Rao B, Wong NC. Ferrous sulfate reduces thyroxine efficacy in patients with hypothyroidism. Ann Intern Med. 1992;117(12):1010–3.
12. Singh N, Singh PN, Hershman JM. Effect of calcium carbonate on the absorption of levothyroxine. JAMA. 2000;283(21):2822–5.
13. Bell DS, Ovalle F. Use of soy protein supplement and resultant need for increased dose of levothyroxine. Endocr Pract. 2001;7(3):193–4.
14. Briesacher BA, Andrade SE, Fouayzi H, Chan KA. Comparison of drug adherence rates among patients with seven different medical conditions. Pharmacotherapy. 2008;28(4):437–43.
15. Guy RH. Transdermal drug delivery. Handb Exp Pharmacol. 2010;197:399–410.
16. Hao Y, Li W, Zhou X, Yang F, Qian Z. Microneedles-based transdermal drug delivery systems: a review. J Biomed Nanotechnol. 2017;13(12):1581–97.
17. Barry BW, Bennett SL. Effect of penetration enhancers on the permeation of mannitol, hydrocortisone and progesterone through human skin. J Pharm Pharmacol. 1987;39(7):535–46.
18. Marwah H, Garg T, Goyal AK, Rath G. Permeation enhancer strategies in transdermal drug delivery. Drug Deliv. 2016;23(2):564–78.
19. Meng S, Zhang C, Shi W, Zhang XW, Liu DH, Wang P, et al. Preparation of osthole-loaded nano-vesicles for skin delivery: characterization, in vitro skin permeation and preliminary in vivo pharmacokinetic studies. Eur J Pharm Sci. 2016;92:49–54.
20. Ramadon D, Mccrudden M, Courtenay AJ, Donnelly RF. Enhancement strategies for transdermal drug delivery systems: current trends and applications. Drug Deliv Transl Res. 2022;12(4):758–91.
21. Stewart SA, Dominguez-Robles J, Utomo E, Picco CJ, Corduas F, Mancuso E, et al. Poly(caprolactone)-based subcutaneous implant for sustained delivery of levothyroxine. Int J Pharm. 2021;607:121011.
22. Ghazi RF, Al-Mayahy MH. Levothyroxine sodium loaded dissolving microneedle arrays for transdermal delivery. Admet Dmpk. 2022;10(3):213–30.
23. Sato E, Yamanishi K, Inui T, Horibe H, Matsumoto A. Acetal-protected acrylic copolymers for dismantlable adhesives with

spontaneous and complete removability. Polymer (Guildf). 2015;64:260–7.
24. Czech Z. Solvent-based pressure-sensitive adhesives for removable products. Int J Adhes Adhes. 2006;26(6):414–8.
25. Zhang X, Liu H, Yue L, Bai Y, He J. Fabrication of acrylic pressure-sensitive adhesives containing maleimide for heat-resistant adhesive applications. Polym Bull (Berl). 2019;76(6):3093–112.
26. Mapari S, Mestry S, Mhaske ST. Developments in pressure-sensitive adhesives: a review. Polym Bull (Berl). 2021;78(7):4075–108.
27. Singh S, Singh J. Transdermal drug delivery by passive diffusion and iontophoresis: a review. Med Res Rev. 1993;13(5):569–621.
28. Williams AC, Barry BW. Penetration enhancers. Adv Drug Deliv Rev. 2004;56(5):603–18.
29. Maurya A, Repka MA, Cegu P, Narasimha MS. Pre-treatment with chemical penetration enhancers in dermal/transdermal drug delivery. J Drug Deliv Sci Technol. 2014;24(3):251–4.
30. Arora A, Prausnitz MR, Mitragotri S. Micro-scale devices for transdermal drug delivery. Int J Pharm. 2008;364(2):227–36.
31. Zorec B, Préat V, Miklavčič D, Pavselj N. Active enhancement methods for intra- and transdermal drug delivery: a review. Slovenian Med J. 2013;82:339–56.
32. Paudel KS, Milewski M, Swadley CL, Brogden NK, Ghosh P, Stinchcomb AL. Challenges and opportunities in dermal/transdermal delivery. Ther Deliv. 2010;1(1):109–31.
33. José JE, Isabel MR, Clara LD. Chemical and physical enhancers for transdermal drug delivery. In: Luca G, editor. Pharmacology. Rijeka: IntechOpen; 2012. p. 19.
34. Mitragotri S. Synergistic effect of enhancers for transdermal drug delivery. Pharm Res. 2000;17(11):1354–9.
35. Saitoh H, Takami K, Ohnari H, Chiba Y, Ikeuchi-Takahashi Y, Obata Y. Effects and mode of action of oleic acid and tween 80 on skin permeation of disulfiram. Chem Pharm Bull (Tokyo). 2023;71(4):289–98.
36. Panchagnula R, Salve PS, Thomas NS, Jain AK, Ramarao P. Transdermal delivery of naloxone: effect of water, propylene glycol, ethanol and their binary combinations on permeation through rat skin. Int J Pharm. 2001;219(1):95–105.
37. Barry BW. Novel mechanisms and devices to enable successful transdermal drug delivery. Eur J Pharm Sci. 2001;14(2):101–14.
38. Kovacik A, Kopecna M, Vavrova K. Permeation enhancers in transdermal drug delivery: benefits and limitations. Expert Opin Drug Deliv. 2020;17(2):145–55.
39. Matos BN, Reis TA, Gratieri T, Gelfuso GM. Chitosan nanoparticles for targeting and sustaining minoxidil sulphate delivery to hair follicles. Int J Biol Macromol. 2015;75:225–9.
40. Kang J, Li X, Liang K, Qi P, Hu X, Li C, et al. Enhancing effect of phosphoric acid on release of loxoprofen sodium in hot-melt pressure-sensitive adhesives based on polystyrene-isoprene-styrene. J Drug Deliv Sci Technol. 2023;88: 104946.
41. Michaelis M, Brummer R, Leopold CS. Plasticization and antiplasticization of an acrylic pressure sensitive adhesive by ibuprofen and their effect on the adhesion properties. Eur J Pharm Biopharm. 2014;86(2):234–43.
42. Cai Y, Tian Q, Liu C, Fang L. Development of long-acting rivastigmine drug-in-adhesive patch utilizing ion-pair strategy and characterization of controlled release mechanism. Eur J Pharm Sci. 2021;161:105774.
43. Lu Y, Chen J, Zhu B, Wang J, Jiang C, Xu M, et al. Effect of oleic acid on the stability and the combustion of nanoaluminium/jp-10 bi-phase system: experimental and molecular dynamics studies. Colloids Surf A. 2023;678:132459.
44. Klähn M, Krishnan R, Phang JM, Lim FCH, van Herk AM, Jana S. Effect of external and internal plasticization on the glass transition temperature of (meth)acrylate polymers studied with molecular dynamics simulations and calorimetry. Polymer (Guildf). 2019;179:121635.
45. Li N, Quan P, Wan X, Liu C, Liu X, Fang L. Mechanistic insights of the enhancement effect of sorbitan monooleate on olanzapine transdermal patch both in release and percutaneous absorption processes. Eur J Pharm Sci. 2017;107:138–47.
46. Guillard EC, Laugel C, Baillet-Guffroy A. Molecular interactions of penetration enhancers within ceramides organization: a ftir approach. Eur J Pharm Sci. 2009;36(2–3):192–9.
47. Moore DJ, Rerek ME. Insights into the molecular organization of lipids in the skin barrier from infrared spectroscopy studies of stratum corneum lipid models. Acta Derm Venereol Suppl (Stockh). 2000;208:16–22.
48. Kumari D, Bhatia E, Awasthi L, Banerjee R. Phospholipid and menthol based nanovesicle impregnated transdermal patch for nutraceutical delivery to diminish folate and iron deficiency. Biomed Mater. 2022;17(4):044101.
49. Anigbogu ANC, Williams AC, Barry BW, Edwards HGM. Fourier transform raman spectroscopy of interactions between the penetration enhancer dimethyl sulfoxide and human stratum corneum. Int J Pharm. 1995;125(2):265–82.
50. Zhang D, Chen B, Mu Q, Wang W, Liang K, Wang L, et al. Topical delivery of gambogic acid assisted by the combination of low-frequency ultrasound and chemical enhancers for chemotherapy of cutaneous melanoma. Eur J Pharm Sci. 2021;166:105975.
51. Wang J, Dong C, Song Z, Zhang W, He X, Zhang R, et al. Monocyclic monoterpenes as penetration enhancers of ligustrazine hydrochloride for dermal delivery. Pharm Dev Technol. 2017;22(4):571–7.
52. Singh I, Morris AP. Performance of transdermal therapeutic systems: effects of biological factors. Int J Pharm Investig. 2011;1(1):4–9.
53. Sugibayashi K, Nakayama S, Seki T, Hosoya K, Morimoto Y. Mechanism of skin penetration-enhancing effect by laurocapram. J Pharm Sci. 1992;81(1):58–64.
54. Ito Y, Ogiso T, Iwaki M. Thermodynamic study on enhancement of percutaneous penetration of drugs by azone[○!R]. J Pharmacobiodyn. 1988;11(11):749–57.
55. Ogiso T, Iwaki M, Bechako K, Tsutsumi Y. Enhancement of percutaneous absorption by laurocapram. J Pharm Sci. 1992;81(8):762–7.
56. Xie F, Chai JK, Hu Q, Yu YH, Ma L, Liu LY, et al. Transdermal permeation of drugs with differing lipophilicity: effect of penetration enhancer camphor. Int J Pharm. 2016;507(1–2):90–101.
57. Zhao H, Lu Y, Zheng J, Xie Y, Li Q. Case report: intraoperative frozen section analysis of thyroid paraganglioma. Front Oncol. 2022;12:1038076.